Polymer Bulletin (2023) 80:6385–6404
https://doi.org/10.1007/s00289-022-04344-6

ORIGINAL PAPER

Flame-retardant synergistic effect of hydroquinone bis(diphenyl phosphate) and tris(2-hydroxyethyl) isocyanurate on epoxy resin

Chaojiu Chen[1] · Shiqian Qin[1] · Xinlong Wang[1] · Tao Luo[1] · Xiuying Yang[1] · Jinyang Wang[1] · Shenggao Yin[1] · Zongpei You[1] · Xinyu Gao[1] · Lin Yang[1]

Received: 11 January 2022 / Revised: 4 May 2022 / Accepted: 13 June 2022 /
Published online: 18 July 2022

Abstract

In this study, epoxy resin (EP) composites were prepared by the incorporation of hydroquinone bis(diphenyl phosphate) (HDP) and tris(2-hydroxyethyl) isocyanurate (THEIC), and the synergistic effects of HDP and THEIC on the flame retardancy of EP were investigated. The flame retardancy of EP composites was systematically evaluated by measuring limiting oxygen index (LOI), UL-94 vertical burning tests and a cone calorimeter. The results indicate that the synergistic effect of the addition of 15% HDP and 15% THEIC in the composite EP-4 is the best. Compared with neat EP, the LOI of EP-4 has increased from 21.7 to 27.5%, and UL-94 reached V-0. The heat release rate (HRR), total heat release (THR), smoke production rate (SPR) and total smoke production (TSP) of EP-4 in the cone calorimeter test decreased by 81.14, 41.42, 72.57 and 53.61%, respectively. The release rates of CO_2 and CO were also significantly reduced, indicating a good synergistic effect between HDP and THEIC. Furthermore, the synergistic flame-retardant mechanism between HDP and THEIC has been thoroughly studied by scanning electron microscopy (SEM) and thermogravimetric analysis/infrared analysis (TG-IR). The results show that HDP/THEIC can effectively strengthen the carbon layer structure resulted from the composite after combustion and increase the flame retardancy of the condensed phase. Meanwhile, PO, PO_2 radicals and NH_3 produced by the degradation of HDP and THEIC are also beneficial to improve the flame retardancy of the gas phase.

Keywords Epoxy resin · Flame retardant · Synergistic effect · Thermogravimetric analysis/infrared spectrometry · Flame-retardant mechanism

✉ Lin Yang
18980632893@163.com

[1] College of Chemical Engineering, Sichuan University, Chengdu 610065, Sichuan, People's Republic of China

Introduction

As an important thermosetting material, epoxy resin (EP) is widely used in adhesives, coatings, microelectronics manufacturing, aerospace and other fields due to its excellent performance, such as superior adhesion, electrical insulation properties, chemical resistance, mechanical strength and processability. Although EP shows such attractive performance, its high flammability still limits its application in many fields [1–3]. Therefore, how to effectively improve the flame retardancy of EP has been an important research direction in the polymer science and engineering community.

In the past, halogenated flame retardants were often used to improve the flame-retardant performance of EP. However, these halogenated flame retardants will release a large number of toxic gases and corrosive substances such as carcinogenic brominated furans, dioxins and hydrogen bromide during combustion [4, 5]. With the increasing attention to environmental problems, the application of halogenated flame retardants has been strictly restricted [6, 7]. Nowadays, high-efficiency halogen-free flame retardants have become the main research direction. In the halogenated-free flame-retardant system, organophosphorus ester flame retardants have the advantages of low toxicity, high efficiency and good compatibility with materials. Thus, they are being considered to replace halogenated flame retardants. In previous studies, there are reported precedents of organophosphorus flame retardants such as bisphenol-A bis(diphenyl phosphate) and triphenyl phosphate that have been applied in epoxy resin [8–10]. However, these flame retardants have relatively low melting points and strong mobility and cannot achieve good effects when used alone. They often need to be applied in conjunction with certain synergists to achieve satisfactory flame-retardant performance effects. As a solid organophosphorus ester flame retardant, hydroquinone bis(diphenyl phosphate) (HDP) has a higher melting point and migration resistance, and as far as the authors know, it has not been used as a flame retardant in epoxy resin, so this study is aimed to investigate it as the epoxy resin flame retardant [11].

In recent years, some triazine compounds have been synthesized and used as charring agents. It has been found that triazine compounds can not only improve the carbon layer structure and enhance the condensed phase flame-retardant effect but also the NH_3 produced by their decomposition can enhance the gas phase flame-retardant effect [12, 13]. Li combined ammonium polyphosphate, melamine, and triazine charring agent to modify the flame retardant of epoxy resin. The combination of triazine charring agent and ammonium polyphosphate can improve the ability of carbon formation during the combustion of EP [14]. Lai synthesized a new triazine-based polymer and combined it with melamine pyrophosphate for flame retardant polypropylene. The results showed that the triazine ring produced by the decomposition of triazine-based polymer can be cross-linked to form a graphite-like char, while the decomposition will also release NH_3 to strengthen the effect of the gas phase flame retardancy [8]. Tris(2-hydroxyethyl) isocyanurate (THEIC) is a derivative of triazine compounds, which

are commonly used as polyvinyl chloride stabilizers, coating intermediates, fuels, and pharmaceuticals. [15, 16] Previously, Li applied ammonium polyphosphate and THEIC as the flame retardants of PP and found that they have a good synergistic effect, which leads to improvement of the limiting oxygen index LOI and UL-94 level of polypropylene and the reduction of the heat release and smoke production during the combustion of polypropylene [17]. It indicates that THEIC has a good effect as a charring agent.

Previously, there have been no attempts to apply HDP and THEIC simultaneously as epoxy flame retardants. Therefore, this study attempted to compound HDP and THEIC into epoxy resin and investigate the flame-retardant synergistic effects of both. Furthermore, the synergistic flame-retardant mechanism between HDP and THEIC has been thoroughly investigated by thermogravimetric analysis (TG), scanning electron microscopy (SEM), thermogravimetric analysis/infrared spectrometry (TG-IR) and Raman spectrometer, etc.

Experimental

Materials

Phosphorus oxychloride ($POCl_3$), hydroquinone, phenol, anhydrous aluminum trichloride, oxalic acid, sodium hydroxide and triethylenetetramine (TETA) were all of the analytical grade and were acquired from Chengdu Jinshan Chemical Reagent Co. Ltd. (China). EP (E-44) was provided by Nantong Xing Chen Synthetic Material Co. Ltd. (China). THEIC was purchased from Bide Pharmatech Co. Ltd. (China).

Preparation of HDP

11.00 g hydroquinone and 76.65 g phosphorus oxychloride were reacted under the catalysis of anhydrous aluminum trichloride at 100 °C for 0.5 h under nitrogen protection, and the excess phosphorus oxychloride was distilled off under reduced pressure to obtain hydroquinone bisphosphorochloride. Hydroquinone bisphosphorochloride reacted with 37.60 g phenol at 120 °C for 4 h. After the reaction, the product was washed with oxalic acid solution and sodium hydroxide solution in turn and finally filtered and dried at 80 °C to obtain the product. [18]

Sample preparation

The EP composites were prepared by a thermal curing process. Firstly, THEIC was added into EP and thoroughly stirred at 80 °C, and then HDP was melted at 100 °C and added into the mixture quickly, stirred well and cooled to 40 °C. Afterward, a certain amount of curing agent TETA was added, and the mixture was left to bubble at room temperature for 10 min initially. Finally, the mixture was poured into a preheated mold at 80 °C and cured at room temperature for 2 h and then cured at

Table 1 Composition and flame retardancy of the samples

Samples	EP (wt%)	HDP (wt%)	THEIC (wt%)	HDP: THEIC	TETA (wt%)	LOI (%)	UL-94
EP	89.3	0	0	–	10.7	21.7	Fail
EP-1	63.5	30	0	–	6.5	25.2	Fail
EP-2	63.5	25	5	5:1	6.5	24.2	Fail
EP-3	63.5	20	10	2:1	6.5	26.3	V-1
EP-4	63.5	15	15	1:1	6.5	27.5	V-0
EP-5	63.5	10	20	1:2	6.5	26.2	V-1
EP-6	63.5	5	25	1:5	6.5	25.5	Fail
EP-7	63.5	0	30	–	6.5	21.4	Fail

80 °C for 4 h. After cooling down, the molds were decoupled to obtain the samples. Table 1 shows the composition samples.

Characterization

The sample size for measuring the LOI value was $127 \times 6.5 \times 3$ mm^3, which was measured on an XZT-100A oxygen index instrument (Kecheng, China). The sample of UL-94 vertical burning tests was performed in a CFZ-3 instrument (Jiangning Analysis Instrument Company, China) with a sample size of $127 \times 12.8 \times 3$ mm^3. LOI test and UL-94 vertical burning tests were carried out according to ASTM D2863-97. The flammability of the sample was evaluated by using a cone calorimeter (FTT iConeR). The sample size was $100 \times 100 \times 5$ mm^3 for the cone calorimeter test, which was carried out according to the test standard of ISO 5560 with a heat flux of 35 KW/m^{2}a.

The thermal stability of the samples was evaluated by a STA449F3 thermal analyzer (NETZSCH, Germany) under a nitrogen atmosphere from 30 to 700 °C using a heating rate of 10 °C/min.

A Vage3 emission scanning electron microscopy (TESCAN, Czech Republic) was used to observe the microstructure of residual char at 20 kV and 500 magnification. The cross-sectional microstructure of the composite was observed at 20 kV and 200 magnification. An IE250 energy-dispersive spectroscopy (Oxford, England) was used to analyze the element content of the sample.

The Raman spectra of the residual chars were measured by a Thermo Scientific DXRxi Raman spectrometer (Thermo Fisher, America) under room temperature from 1000 to 2000 cm^{-1} with a 450 nm argon laser line excitation source.

A TG-IR instrument comprised the STA449F3 thermal analyzer (NETZSCH, Germany) and a Fourier spectrometer (PerkinElmer, America). The test conditions were in the wavenumber range from 650 to 4000 cm^{-1} and raised from 30 to 800 °C under an air condition.

Fourier-transformed infrared spectra (FTIR) of the residual chars were obtained by using a Fourier infrared spectrometer (PerkinElmer, America) in the wavenumber range from 400 to 4000 cm^{-1}.

Tensile and flexural tests of the sample were carried out on 119 INSTRON universal testing machines (Instron, America) with two different sizes, $180 \times 20 \times 4$ mm^3 and $80 \times 15 \times 4$ mm^3, respectively. The tensile and flexural tests were performed according to GB/T 2567–2008 (China).

Results and discussion

Flame retardancy of EP composites

Analysis of LOI and UL-94 results

The effect of different ratios of HDP/THEIC on the flame retardancy of EP is shown in Table 1 and Fig. 1. The results show that the LOI value of neat EP is 21.7% and no rating in the UL-94 test. The LOI value of EP-7 with 30 wt% THEIC only is 21.4%. The LOI value of EP-1 with 30 wt% HDP reached 25.2%, but cannot improve the UL-94 level. The LOI value of the remaining samples shows a pattern of increasing and then decreasing as the amount of THEIC increases, and the same for the UL-94 test. The LOI value of the EP-4 with 15 wt% HDP and 15 wt% THEIC reached up to 27.5% along with a V-0 rating in the UL-94 test, increased by 26.7% compared to neat EP. It can be seen that there is a good synergy between HDP and THEIC, and the effect of the synergy was related to the ratio of addition. There is a good synergistic effect between HDP and THEIC. The possible reason is that HDP can well catalyze the dehydration of THEIC to carbon, so as to increase the residual char amount of the material after combustion, and THEIC can also decompose NH3, thereby strengthening the gas phase flame-retardant effect, and further research is

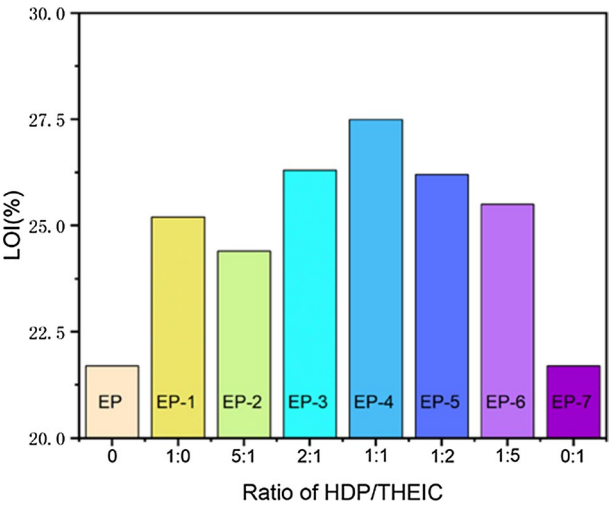

Fig. 1 The effect of HDP/THEIC weight ratios on the limiting oxygen index (LOI) of composite epoxy resin samples

needed. In order to better explore the synergistic effect between HDP and THEIC, more in-depth research is necessary. EP-4 has the best flame-retardant effect and can best reflect the synergistic effect between HDP and THEIC. Therefore, the subsequent analysis will focus on comparing the differences between EP-4 and EP.

Analysis of cone calorimeter test results

The cone calorimeter test has a good correlation with real fires and is considered the best means to characterize the real burning situation of materials. It can obtain some parameters that can be related to the burning behavior of materials in a fire, parameters include heat release rate (HRR), total heat release (THR), smoke production rate (SPR) and total smoke production (TSP), CO release rate and CO_2 release rate [19]. According to UL-94 and LOI test results, EP-4 had the best flame-retardant effect and could better reflect the synergistic effect between HDP and THEIC. Therefore, EP-4 and EP were selected for comparison in the cone calorimeter test. The data obtained from the tests are shown in Fig. 2 and Table 2.

It can be seen from Fig. 2a, b that the HRR increases rapidly with a peak HRR (pHRR) value of 1553.16 kW/m^2, and the THR reaches 107.66 MJ/m^2 once the EP is ignited. These results show that the combustion of EP rapidly exerts heat and releases a large amount of heat at the same time. In contrast, the pHRR of the EP-4 sample is obviously decreased, being only 292.92 kW/m^2 and 81.14% lower than the pHRR of EP, and the THR is only 63.07 MJ/m^2 and 41.42% lower than the THR of EP. The simultaneous introduction of HDP and THEIC can effectively reduce the heat release rate and total heat release of the composite EP samples.

In the case of a fire, intense smoke is often the primary cause of fatalities, so it is especially important to reduce the smoke amount generated by combustion. Figure 2c, d shows the graphs of TSP and SPR for the EP and EP-4 samples. It can be seen that the combustion of the EP sample exhibited high peak SPR (pSPR) and TSP, indicating that a lot of flue gas was produced. The pSPR of the EP-4 sample is only 0.0961 m^2/s and the TSP is 16.88 m^2, with a decrease of 72.57 and 53.61%, respectively. In addition, the release of CO_2 and CO in the smoke is also suppressed (Fig. 2e, f), the peak release rate of CO_2 and CO of the EP samples is 1.067 and 0.0855 g/s, respectively. While the release rate of CO_2 and CO of the EP-4 sample is significantly lower, the peak release rate is 0.219 and 0.0314 g/s, respectively. The SPR, TSP, and release rate of CO_2 and CO during the combustion of the composites are significantly reduced, indicating that the simultaneous addition of HDP and THEIC can effectively reduce the smoke generation during combustion.

It is worth noting that the HRR, SPR, CO release rate, and CO_2 release rate profiles of both the EP and EP-4 samples show two peaks, and the advent time of the second peak for the EP sample is always earlier than that of the EP-4 sample. The reason for this observed phenomenon might be that the first peak belongs to the thermal decomposition of EP itself, and the second peak represents the further decomposition of the carbon layer produced by combustion. In Fig. 3, by comparing the residual carbon of the two samples, it can be found that only a small amount of residual carbon remains after the combustion of the EP sample, while the combustion of the EP-4 sample forms a huge layer of expanded carbon materials. This

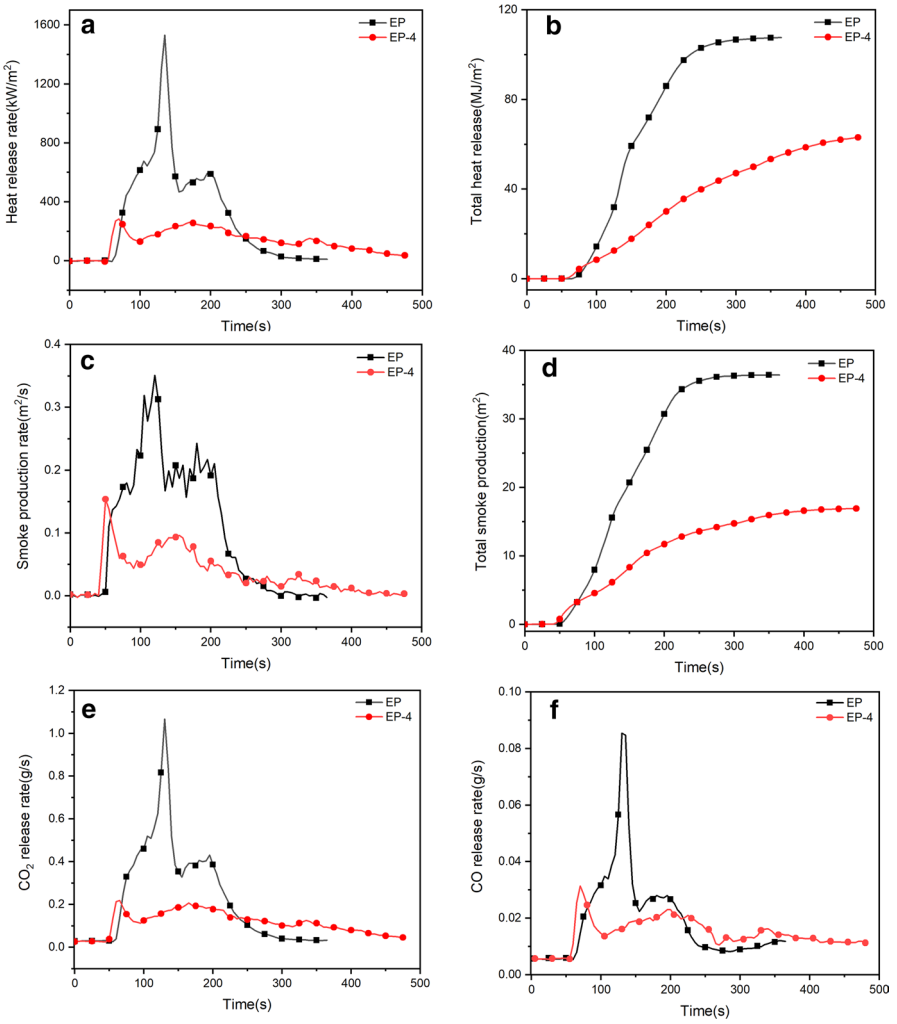

Fig. 2 HRR (**a**), THR (**b**), SPR (**c**), TSP (**d**), CO_2 release rate (**e**) and CO release rate (**f**) of curves

Table 2 Combustion parameters obtained from cone calorimeter

Samples	TTI (s)	t-pHRR (s)	pHRR(kW/m^2)	THR(MJ/m^2)	pSPR (m^2/s)	TSP (m^2)	FPI (sm^2/kW)	FGI (kW/m^2/s)
EP	51	135	1553.16	107.66	0.35	36.39	0.033	11.50
EP-4	42	70	292.92	63.07	0.096	16.88	0.14	4.18

indicates that the residual carbon formed by the combustion of EP is completely decomposed, but the combustion of EP-4 results in a fluffy carbon layer that is well insulated from heat and can thus slow down the decomposition. So, the second peak

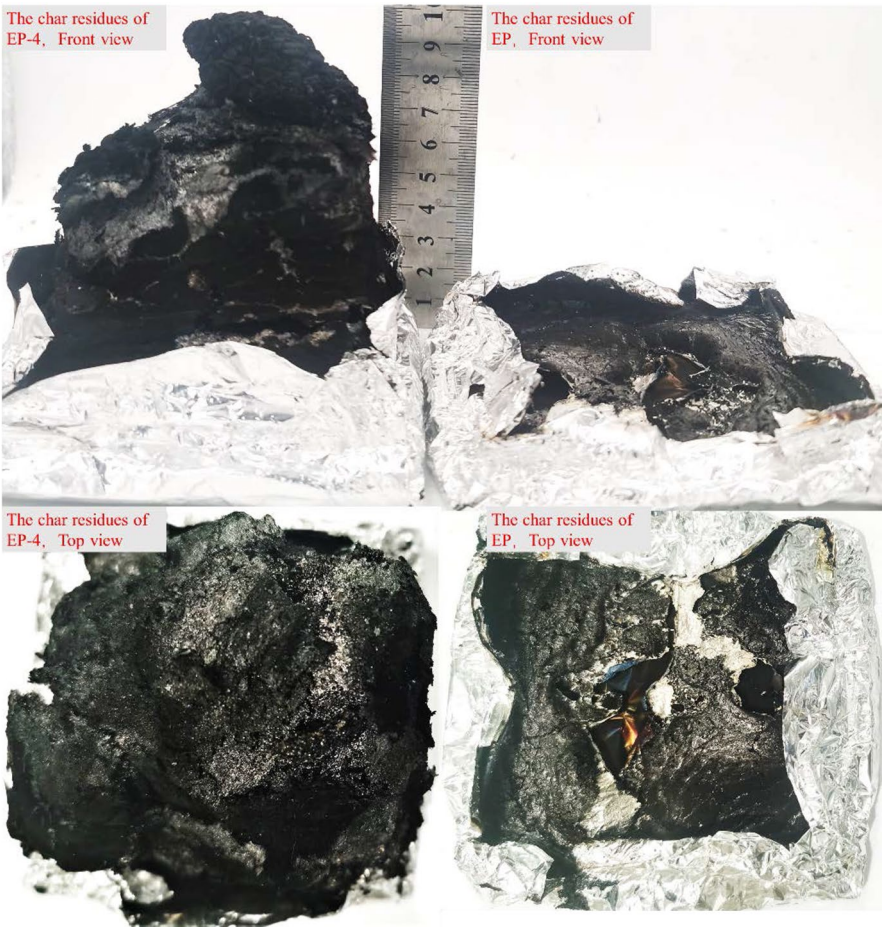

Fig. 3 Digital photographs of the char residues of EP and EP-4 after the cone calorimeter test

reached comes later. In addition, the expanded carbon layer effectively blocks the heat and material exchange between the matrix and the burning area. This is the reason for the decrease in HRR, THR, SPR, TSP, and CO_2 and CO release rate of the composite. This further indicates that HDP and THEIC have a good synergistic effect.

In order to give a comprehensive evaluation of the fire safety effects of the composites, the fire performance index (FPI) and fire growth index (FGI) were calculated for both; the results are shown in Table 2. FPI is defined as the time to ignition (TTI) divided by pHRR. A higher FPI suggests that there is more time for rescue before the violent combustion. FGI is expressed as the pHRR divided by the time to pHRR. A higher FGI represents that the material can be easily ignited and reach a higher pHRR [20, 21]. The FPI of EP and EP-4 is 0.033 and 0.14 sm^2/kW, respectively, and the FGI is 11.50 and 4.18 $kW/m^2/s$, respectively. With the incorporation

of HDP and THEIC into EP, the FPI of the EP-4 sample is increased and the FGI is decreased, indicating that the fire safety performance of the composites has been improved.

Thermal stability

The thermogravimetric analysis (TGA) curves and derivative thermogravimetric (DTG) curves for all samples are shown in Fig. 4 and Table 3. The temperature corresponding to a 5% weight loss of the material is defined as the onset decomposition temperature (T_{onset}). The temperature at the maximum weight loss rate is defined as the fastest decomposition temperature (T_{max}) [22].

The decomposition of EP is very fast, featuring only a one-step decomposition. The T_{onset} and T_{max} appear at 333.8 and 371.9 °C, respectively. The decomposition is basically finished at 500 °C, and there is only 11.80% of the initial mass residue left behind at 700 °C. The thermal decomposition of HDP mainly occurs between 250 and 450 °C, and the T_{onset} and T_{max} appear at 277.5 and 354.6 °C, respectively. In addition, there is still a small weight loss process near 540 °C. This is because the decomposition of HDP occurs in two steps; the first step is caused by the breakage of HDP's own structure, while the decomposition at 540 °C is caused by the further

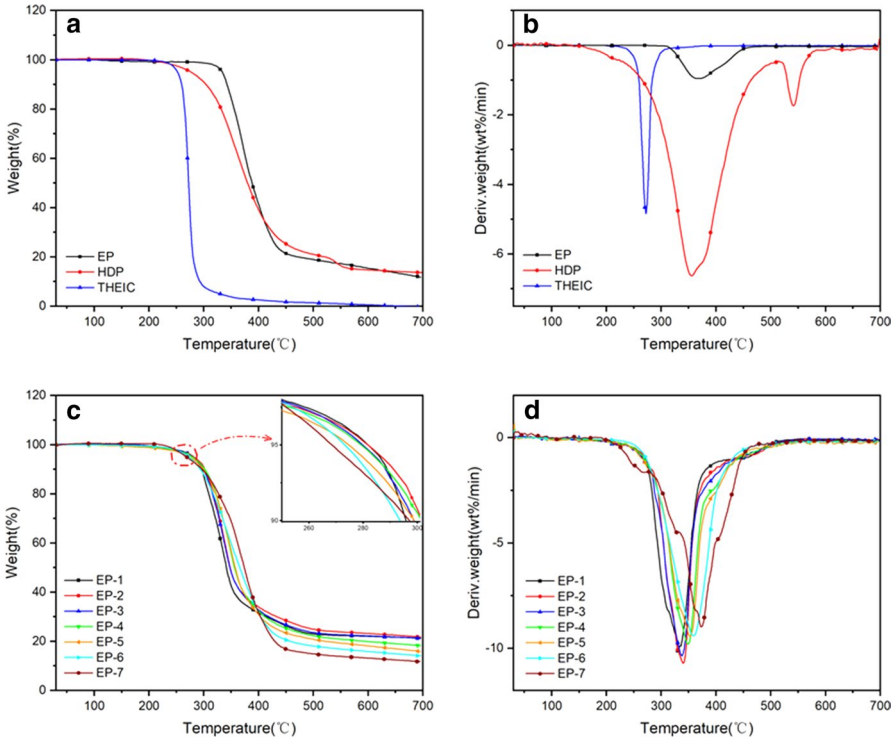

Fig. 4 TGA and DTG curves for EP, HDP, THEIC (**a**, **b**), and EP composites (**c**, **d**)

Table 3 Data from TGA and DTG curves of EP, HDP, THEIC, and EP composites

Samples	T_{onset} (°C)	T_{max} (°C)	W_{exp} (wt%)
EP	333.8	371.9	11.80
HDP	277.5	354.6	13.64
THEIC	252.2	271.4	0
EP-1	281.9	331.2	21.13
EP-2	281.8	340.1	21.72
EP-3	279.7	338.8	21.26
EP-4	279.4	349.1	18.17
EP-5	274.7	352.8	15.82
EP-6	273.3	359.3	14.05
EP-7	268.5	273.1 and 373.7	11.71

dehydration and decomposition of polyphosphoric acid [11, 23]. There is 13.64% mass residue at 700 °C. The decomposition of THEIC is only one step that occurs within the temperature range of 250 to 400 °C, and the decomposition is complete without any mass residue.

The TGA curves and DTG curves of the composites are shown in Fig. 4c, d, and all the samples showed a similar decomposition process, which was concentrated mainly occurs between 200 and 500 °C.

As shown in Table 3, the T_{onset} of the EP composites is significantly lower than that of the neat EP, which is caused by the lower decomposition temperature of HDP and THEIC. The T_{onset} of all composites decreases as the percentage of THEIC increases, which is due to the lower T_{onset} of THEIC than HDP. Thus, the added THEIC amount has a greater effect on the T_{onset}.

It is noteworthy that the DTG curve of sample the EP-7 sample shows two obvious peaks at both 273.1 and 373.7 °C, respectively. The first weight loss peak is due to the decomposition of THEIC, and the second peak at 373.7 °C is due to the decomposition of EP. This indicates that adding THEIC alone will only accelerate the decomposition of composites. For the EP-1 sample, the T_{max} appears at 331.2 °C. In comparison, HDP compounded with THEIC results in a higher T_{max}, which indicates that the combination of HDP and THEIC can increase the decomposition of the sample.

Comparing the final mass residues of all samples, it can be found that the mass residues of all samples showed first increase and decrease with the ratio of THEIC. Only the EP-2 and EP-3 samples have more mass residues than the EP-1 sample, other samples have fewer mass residues, but the EP-2 ~ EP-6 samples have more mass residues than the EP-7 sample. This indicates that THEIC has a certain carbon formation ability effect after being combined with HDP. Theoretically, the amount of residues char is generally linked to the flame-retardant effect of the composites. However, it is true that the EP-4 sample has the best flame-retardant effect, indicating that the amount of residual char from the decomposition of the sample cannot entirely reflect the synergistic effect between THEIC and HDP, and further research is needed.

Condensed phase analysis

Microstructures of the residual chars

The flame-retardant effect of the material is not only related to the number of residual char yields but is also related to the microstructure of the residual carbon. To further study the synergistic effect between HDP and THEIC and the flame-retardant mechanism of the condensed phase, the microstructure of the residual char was characterized by SEM. Figure 5 shows the microscopic morphology of the residual chars after the combustion of each composite.

The results confirm that the microstructure of the residual chars is closely related to the ratio of HDP and THEIC. The residual chars from EP (a) are full of fissures and have a broken structure. The residual chars of EP-1 (Fig. 5b) are loose and fragmented when only HDP is added, while the residual chars of EP-7 (Fig. 5h) are dense but with large pores when only THEIC is added, and such a residual char structure is not conducive to slowing down the heat and mass transfer between the unburned matrix and the combustion zone. When HDP and THEIC are added in different ratios, the structure of the residual chars is significantly changed. As the

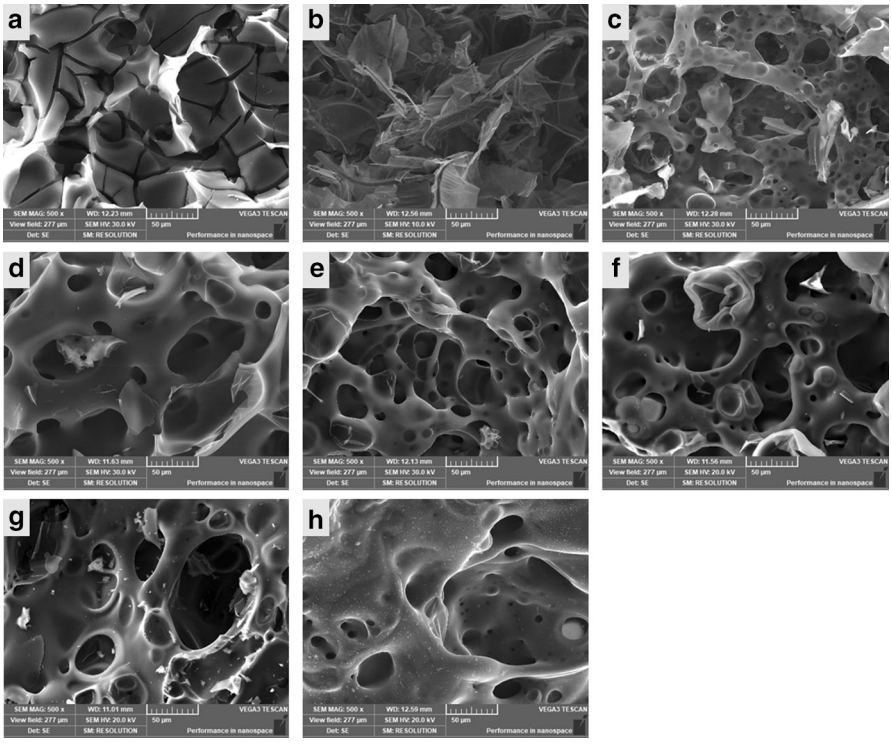

Fig. 5 SEM images of the residual char of EP (**a**), EP-1 (**b**), EP-2 (**c**), EP-3 (**d**), EP-4 (**e**), EP-5 (**f**), EP-6 (**g**), EP-7 (**h**)

ratio of THEIC increases, the residual chars gradually become dense and form uniform pores in the carbon layer (EP (Fig. 5c) ~ EP (Fig. 5g)). This is because HDP produces phosphoric acid derivatives during the thermal decomposition, to catalyze the transformation of THEIC and other hydroxyl-containing compounds from EP decomposition into carbon. Meanwhile, the decomposition of THEIC will produce NH_3, which will leave cavities in the residual chars. However, as with the increase of the THEIC ratio, a large amount of NH_3 is generated, which leads to the expansion of pore channels and finally structural damage in the carbon layer. A stable residual char structure can ensure that the carbon layer will not be broken during combustion. The uniform pore channels can isolate the heat generated by the combustion and retain the non-combustible gases produced by the decomposition, dilute the air and prevent further decomposition of the material. It can be seen from Fig. 5 that the char from EP-4 (Fig. 5e) has alveolate structures, and the size and distribution are the most uniform compared to other samples. Therefore, this illustrates the reason why the amount of residual chars from the EP-4 sample is not the highest, but it can bring the best flame-retardant effect among those samples.

Raman spectroscopy can effectively characterize the graphitization degree of the residual chars. The characteristic peaks at 1358 and 1580 cm^{-1} in the spectra are called D-peak and G-peak, respectively, which represent the vibration of amorphous carbon and crystalline graphite, respectively. Therefore, the ratio of the integrated peak intensity of D to G peak (I_D/I_G) can indicate the graphitization degree of the residual chars, and a lower I_D/I_G value indicates a higher graphitization degree of the residual carbon and a better thermal insulation effect [24, 25]. Figure 6 shows the Raman spectra of the residual chars of EP and EP-4. The I_D/I_G value of the EP-4 sample is 1.403, smaller than that of the EP sample being at 1.865. The results indicate that the addition of HDP and THEIC can increase the degree of graphitization of the residual carbon, thereby enhancing the strength of the carbon layer. Then, a stronger carbon layer can better isolate the heat transfer and avoid further decomposition of the composites.

In conclusion, the combination of THEIC and HDP can increase the graphitization degree of the residual chars and strengthen the structure of the carbon layer. The decomposition of THEIC will also produce NH_3 to form uniform pores in the

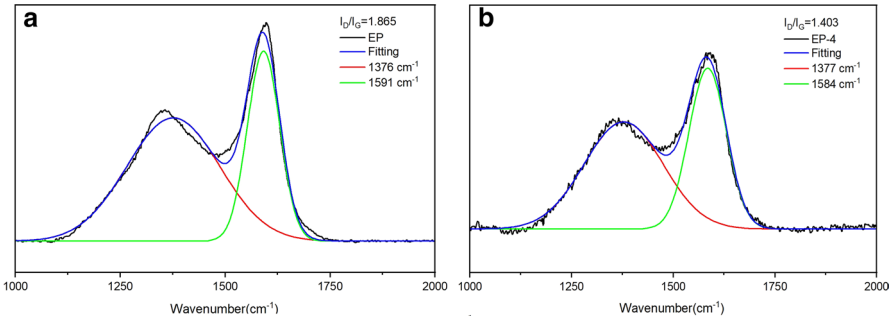

Fig. 6 Raman spectrum of residual carbon of EP (**a**), EP-4 (**b**)

carbon layer. The dense and porous carbon layer effectively enhances the condensed phase flame-retardant effect of the material and reduces the mass and heat exchange between the composites and the combustion area, thus enhancing the flame-retardant performance of the composites.

Chemical composition of the residual char

EP-4 has the best flame-retardant effect and can best reflect the synergistic effect between HDP and THEIC. Therefore, EP-4 and EP were selected as a comparison to study the difference in the chemical composition of residual carbon. Figure 7 shows the comparison of the elemental composition of the EP-4 before and after the combustion. The presence of N is clear in the EP-4 sample before burning, which is caused by the addition of THEIC. However, N was no longer detected in the sample after combustion, indicating that all N atoms in THEIC were released in the form of gas. In addition, the contents of C and P in the residual char increase, but the content of O decreases. This indicates that a part of the P remains in the residual carbon. This may be a plausible reason for the observed phenomenon: Phosphoric acid derivatives released from the decomposition of HDP are involved in the dehydration of the material into carbon during combustion, which releases water into the air. So, it leads to the decrease of the O content and the increase of the P content. The

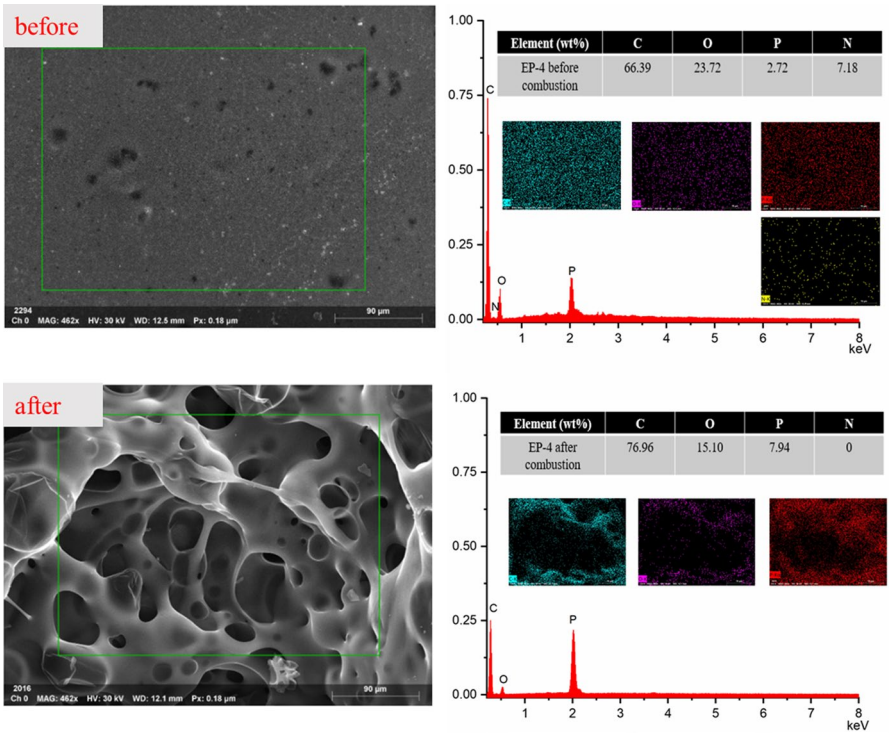

Fig. 7 SEM image and elemental analysis of the EP-4 sample before and after combustion

increase of the C content indicates that the carbon layer formed effectively protects the material and prevents further decomposition.

Figure 8 shows the spectra of the residual char, which gives a further proof of the chemical compositions of the carbon layer. The absorption peaks around 1600 and 1236 cm^{-1} are attributed to the C=C and C–C stretching vibrations of aromatic compounds. Besides, there are some additional absorption peaks present in the residual carbon IR spectrum of the residual carbon from the EP-4 sample, including the P=O groups (around 1165 cm^{-1}), P–O groups (around 1080 and 752 cm^{-1}), and P–O–C groups (around 985 cm^{-1}). This indicates that the phosphate derivatives from the HDP decomposition catalyze the conversion of EP and THEIC to organophosphates with aromatic structures during the combustion and the char layer is mainly composed of graphite-like complexes, with aromatic structures bridged by P–O–C groups [8, 22, 26].

Gas phase analysis

To further investigate the gas-phase mechanism, a TG-IR analysis of the EP and EP-4 samples was carried out under air conditions. Figure 9 shows the IR spectra of the decomposition products of the EP and EP-4 samples at different temperatures.

The characteristic peaks of typical thermal decomposition products of epoxy resin were observed at 3500 ~ 4000 cm^{-1}, 2800 ~ 3100 cm^{-1}, 2400 ~ 2200 cm^{-1}, 2200 ~ 2000 cm^{-1}, 1735 and 1172 cm^{-1} [27]. The peaks at 3500 ~ 4000 cm^{-1} belong to the vibration of O–H groups, which are from phenols and water produced by the EP decomposition. The peaks at 2800 ~ 3100 cm^{-1} belong to $–CH_2–$,

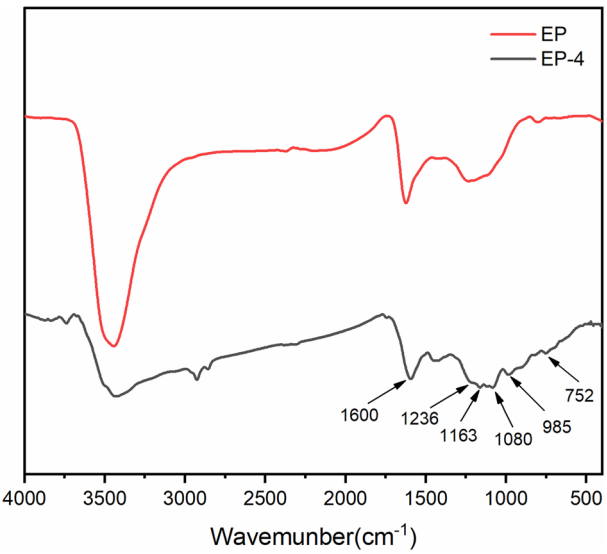

Fig. 8 FTIR spectra of the residual char form EP and EP-4

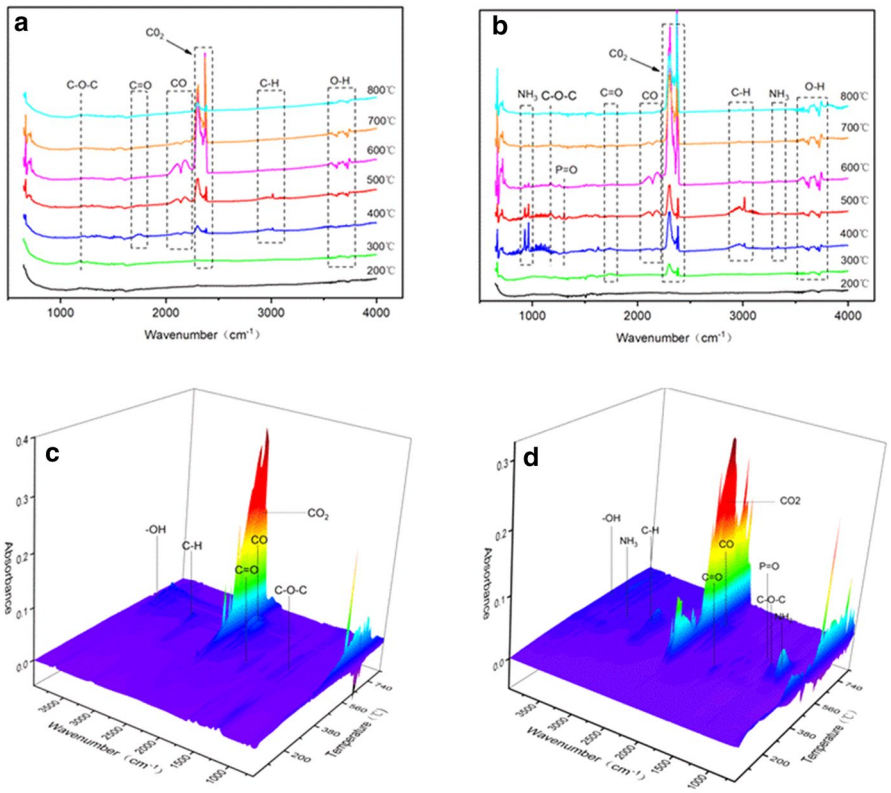

Fig. 9 FTIR spectra of the pyrolysis products at different temperatures (**a**, **b**) and 3D TG-FTIR profiles (**c**, **d**) obtained for the EP (left column) and EP-4 (right column)

–CH_3 produced by hydrocarbon pyrolysis. The peaks at 2400 ~ 2200 cm^{-1} and 2200 ~ 2000 cm^{-1} were related to the characteristic peaks of CO_2 and CO, respectively. The peaks at 1735 and 1172 cm^{-1} are attributed to C=O and C–O–C groups. The spectra of the EP and EP-4 decomposition products are similar. In addition to the above typical absorption peaks, the absorption peaks at 1304 cm^{-1} are related to P=O. The absorption peaks at 3332, 965, and 930 cm^{-1} corresponded to NH_3 produced by the decomposition [28]. This proves that all N atoms in THEIC are released in the form of NH_3. In summary, PO, PO_2 radicals and NH_3 will be produced during the combustion of EP-4. NH_3, CO_2, and H_2O can dilute ambient oxygen, and the PO and PO_2 radicals generated by the decomposition can react with H and OH to terminate the radical chain generated during the combustion, which inhibits further decomposition of the material and thus has a quenching effect. The results of TG-IR analyses show that the introduction of HDP and THEIC renders the composites also a gas-phase flame-retardant mechanism.

Flame-retardant mechanism

Based on the results obtained, a possible flame-retardant mechanism is proposed for the combined HDP and THEIC system, as shown in Fig. 10.

In the condensed phase, the decomposition of HDP produces phosphate derivatives, which can catalyze the dehydration of THEIC and the hydroxyl-containing compounds produced by the decomposition of EP to form a dense carbon layer, thus inhibiting further combustion of the material. In the gas phase, the decomposition of HDP and THEIC can produce CO_2, H_2O, NH_3 and other non-combustible gases to dilute the combustible gas and oxygen. In addition, PO and PO_2 radicals are produced during the decomposition of HDP can react with a large number of active radicals (H and OH) produced by the decomposition of EP to slow down the further decomposition of the material. Moreover, the gas can make the carbon layer porous and strengthen the flame-retardant effect of the condensed phase. In conclusion, the flame-retardant mechanism of the combined HDP and THEIC system is a synergistic combination of condensed phase and gas phase flame-retardant mechanisms.

Mechanical properties

Analysis of the cross-sectional morphology of composites

The compatibility of flame retardant and epoxy resin can be analyzed by observing the cross-sectional morphology of the composite. Figure 11 shows the cross-sectional morphology of all samples. It can be seen that the cross-sectional morphology of EP is relatively smooth, and there are only a few folds on the section. The same is true when only HDP is added, indicating that HDP has good compatibility with EP.

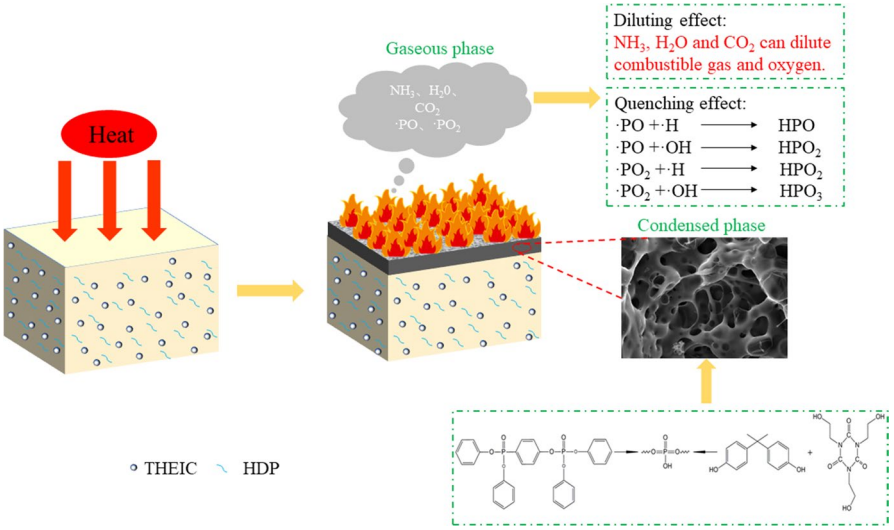

Fig. 10 Schematic of the flame-retardant mechanism of EP-4

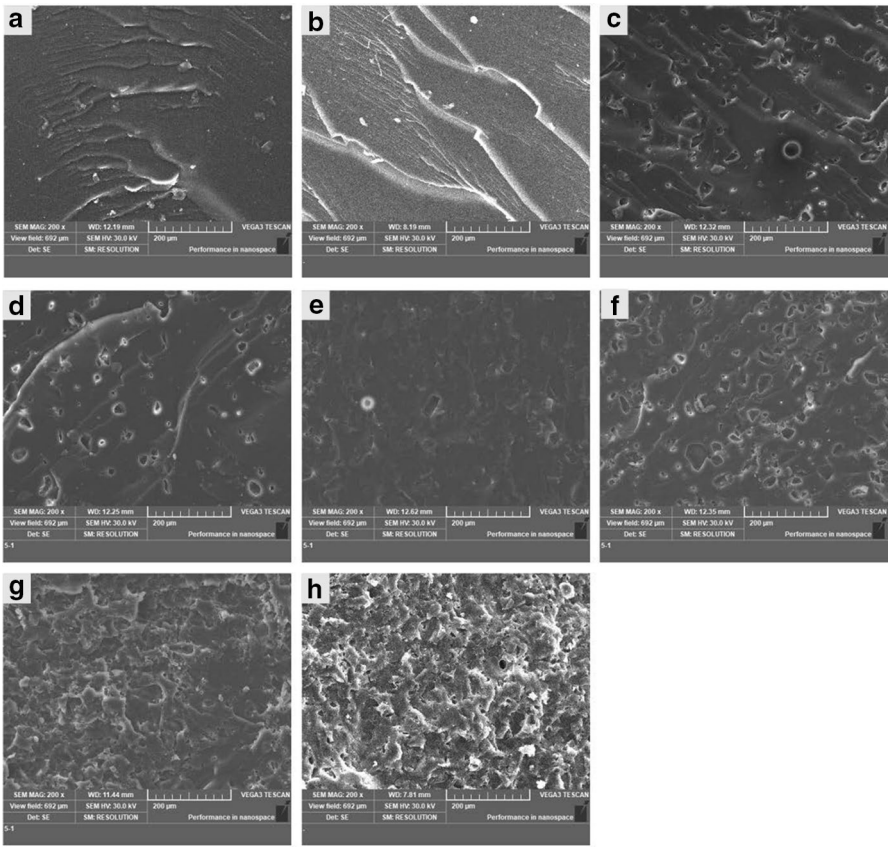

Fig. 11 SEM images of cross-sectional morphology of EP (**a**), EP-1 (**b**), EP-2 (**c**), EP-3 (**d**), EP-4 (**e**), EP-5 (**f**), EP-6 (**g**), EP-7 (**h**)

However, with the increase of THEIC ratio, the cross-sectional morphology of the composites becomes rough, indicating that the compatibility between THEIC and EP is poor. The addition of THEIC will affect the mechanical properties of the composites to a certain extent.

Analysis of tensile and flexural tests results

Tensile and flexural tests were used to further analyze the effect of HDP and THEIC addition on the mechanical properties of composites. Figure 12 shows the comparison of tensile and flexural properties of samples with different HDP/THEIC weight ratios.

It can be observed that the tensile and flexural strengths of the samples decrease with the increase of the THEIC ratio, while the tensile and flexural modulus show an increasing trend in general. The decrease in strength indicates that the addition of THEIC reduces the maximum stress that the material can withstand when subjected

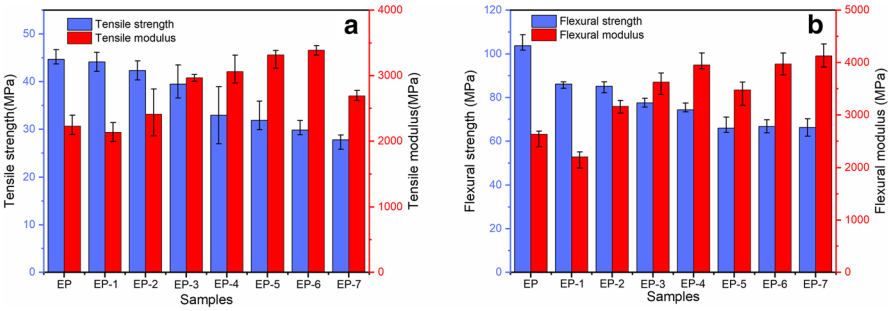

Fig. 12 The effect of different HDP: THEIC weight ratios on the mechanical properties of the composites

to deformation, while the increase in modulus indicates that the rigidity of the composites increases and less deformation occurs when an external force is applied. The increase in modulus is possibly due to the rigidity of THEIC being higher than that of neat EP. When the rigidity of the particles is higher than the matrix, its addition to the matrix can increase the modulus of the composites. The tensile and flexural strengths of the EP sample are 44.70 and 103.72 MPa, respectively, and the tensile and flexural strengths of the EP-4 sample, the one with the best flame-retardant property is 32.93 and 74.42 MPa, respectively, each with a decrease of 26.33 and 28.25%, respectively, as compared to EP. This is because that THEIC is added in a solid form and does not blend well with EP, thus leading to a decrease in the tensile and flexural strength of the material [29]. The compatibility of THEIC with EP needs to be improved to reduce the effect of THEIC on the mechanical properties of the material. Chemical modification of THEIC may improve its compatibility with EP.

Conclusions

HDP and THEIC were added to the epoxy resin, and the flame-retardant synergistic effect was investigated. THEIC and HDP show excellent synergistic flame-retardant effects. The LOI value of the EP-4 sample with 15 wt% HDP and 15 wt% THEIC reaches up to 27.5% increased by 26.7% compared to neat EP. Also, the flame retardancy of the EP-4 sample reaches a V-0 rating in the UL-94 test. The results of the cone calorimeter test showed that HRR, THR, SPR, TSP, CO_2 release rate, and CO release rate are all significantly reduced.

The analyses of the residual chars and released gases after the combustion of the EP composites show that the introduction of HDP and THEIC facilitates the formation of uniform cavities in the carbon layer, which can effectively hinder the heat and material exchange between the composite and the combustion area and enhances the condensed phase flame-retardant effect. Moreover, NH_3, CO_2, H_2O, PO^- and PO_2^- radicals generated by the decomposition of the composites effectively improve the gas phase flame-retardant effect. These results prove that the flame-retardant

mechanism of the EP composites contains the condensed phase and the gas phase actions simultaneously. However, the addition of THEIC will have some influence on the mechanical properties of EP composites. The reason for this phenomenon is that THEIC is added to EP in the form of solid particles, which has poor compatibility with EP. Microencapsulation of THEIC and its addition to EP may achieve good results.

Funding Natural Science Foundation of China, 32172677, XinLong Wang.

References

1. Chu F, Ma C, Zhang T et al (2020) Renewable vanillin-based flame retardant toughening agent with ultra-low phosphorus loading for the fabrication of high-performance epoxy thermoset. Compos Part B-Eng 190:107925
2. Liu J, Dai J, Wang S et al (2020) Facile synthesis of bio-based reactive flame retardant from vanillin and guaiacol for epoxy resin. Compos Part B-Eng 190:107926
3. Jin F-L, Li X, Park S-J (2015) Synthesis and application of epoxy resins: a review. J Ind Eng Chem 29:1–11
4. Lu SY, Hamerton I (2002) Recent developments in the chemistry of halogen-free flame retardant polymers. Prog Polym Sci 27:1661–1712
5. Bai Z, Jiang S, Tang G et al (2014) Enhanced thermal properties and flame retardancy of unsaturated polyester-based hybrid materials containing phosphorus and silicon. Polym Adv Technol 25:223–232
6. Yu G, Bu Q, Cao Z et al (2016) Brominated flame retardants (BFRs): a review on environmental contamination in China. Chemosphere 150:479–490
7. Yang S, Wang J, Huo S et al (2015) Synthesis of a phosphorus/nitrogen-containing additive with multifunctional groups and its flame-retardant effect in epoxy resin. Ind Eng Chem Res 54:7777–7786
8. Lai X, Zeng X, Li H et al (2012) Synergistic effect between a triazine-based macromolecule and melamine pyrophosphate in flame retardant polypropylene. Polym Compos 33:35–43
9. Baek HH, Lee JY, Hong SH et al (2004) Thermal properties and microencapsulation of a phosphate flame rtardant with a epoxy resin. Polym-Korea 28:404–411
10. Gao M, Sun Y (2013) Flame retardancy and thermal degradation behaviors of epoxy resins containing bisphenol abis(diphenyl phosphate) oligomer. Polym Eng Sci 53:1125–1130
11. Ren Y, Fu Q, Wang X et al (2015) Fire retardant synergism of hydroquinone bis(diphenyl phosphate) and novolac phenol in acrylonitrile-butadiene-styrene copolymer. Fire Mater 39:557–569
12. Chen W, Yuan S, Sheng Y et al (2015) Effect of charring agent THEIC on flame retardant properties of polypropylene. J Appl Polym Sci 132:41214
13. Wang W, Wang Z (2021) Flame retardancy, thermal decomposition and mechanical properties of epoxy resin modified with copper N, N'-piperazine (bismethylene phosphonate). J Therm Anal Calorim 147:2155–2169
14. Xiang Li, Runhua Chen, Yi Wei et al (2021) Flame retardant epoxy resins and glass fiber reinforced epoxy composites synergistically modified by ammonium polyphosphate, melamine and triazine carbon-forming agent. Acta Mater Compos Sin 38(09):2796–2806
15. Lewin M, Endo M (1995) Intumescent systems for flame retarding of polypropylene. Fire Polym II:91–116
16. Nalepa RW, Scharf DJ (1993) Three-component intumescent flame retardant. US5204393
17. Qiang LY, Fen HQ, Wei YJ et al (2013) Synergistic flame retardancy of Type II ammonium polyphosphate and 1,3,5-Tr (2-hydroxyethyl) cyanuric acid in polypropylene. J Qingdao Univ Sci Technol 34:231–235
18. Fu QJ, Wang XL, Zhang ZY et al (2013) Synthesis and application of phosphorus flame retardant HDP on ABS composites. Acta Polym Sin 02:166–173

19. Ai L, Chen S, Yang L et al (2021) Synergistic flame retardant effect of organic boron flame retardant and aluminum hydroxide on polyethylene. Fiber Polym 22:354–365
20. Fang S, Hu Y, Song L et al (2007) Mechanical properties, fire performance and thermal stability of magnesium hydroxide sulfate hydrate whiskers flame retardant silicone rubber. J Mater Sci 43:1057–1062
21. Nazaré S, Kandola B, Horrocks AR (2002) Use of cone calorimetry to quantify the burning hazard of apparel fabrics. Fire Mater 26:191–199
22. Zhao W, Liu J, Peng H et al (2015) Synthesis of a novel PEPA-substituted polyphosphoramide with high char residues and its performance as an intumescent flame retardant for epoxy resins. Polym Degrad Stab 118:120–129
23. Chen L, Yang Z, Ren Y-y et al (2015) Fourier transform infrared spectroscopy-thermogravimetry analysis of the thermal decomposition mechanism of an effective flame retardant, hydroquinone bis(di-2-methylphenyl phosphate). Polym Bull 73:927–939
24. Wang J, Tang H, Yu X et al (2021) Reactive organophosphorus flame retardant for transparency, low-flammability, and mechanical reinforcement epoxy resin. J Appl Polym Sci 138:50536
25. Fu H, Cui Y, Lv J (2019) Fire retardant mechanism of PA66 modified by a "trinity" reactive flame retardant. J Appl Polym Sci 137:47488
26. Wang K, Liu H, Wang C et al (2021) Flame-retardant performance of epoxy resin composites with SiO_2 nanoparticles and phenethyl-bridged DOPO derivative. ACS Omega 6:666–674
27. Zhao P, Zeng W, Yang Z et al (2021) Preparation of a novel functionalized magnesium-based curing agent as an intrinsic flame retardant for epoxy resin. Chemosphere 273:129658
28. Cheng J, Duan H, Yang S et al (2020) A P/N-containing flame retardant constructed by phosphaphenanthrene, phosphonate, and triazole and its flame retardant mechanism in reducing fire hazards of epoxy resin. J Appl Polym Sci 137:49090
29. Yang J-W, Wang Z-Z (2018) Synthesis of aluminum ethylphenylphosphinate flame retardant and its application in epoxy resin. Fire Mater 42:638–644